Rock and Soil Mechanics

Volume 42 | Issue 8 Article 5

12-16-2021

Experimental study on the stress wave attenuation effect of filled cracks in rocks under confining pressure

Xin LIU

Hong-fa XU

Peng-xian FAN
fan-px@139.com

Han-sheng GENG

See next page for additional authors

Custom Citation

LIU Xin, XU Hong-fa, FAN Peng-xian, GENG Han-sheng, MO Jia-quan, WANG De-rong. Experimental study on the stress wave attenuation effect of filled cracks in rocks under confining pressure[J]. Rock and Soil Mechanics, 2021, 42(8): 2099-2108.

Experimental study on the stress wave attenuation effect of filled cracks in rocks under confining pressure

Authors

Xin LIU, Hong-fa XU, Peng-xian FAN, Han-sheng GENG, Jia-quan MO, and De-rong WANG

Rock and Soil Mechanics 2021 42(8): 2099−2108 ISSN 1000−7598
https: //doi.org/10.16285/j.rsm.2021.5076 rocksoilmech.researchcommons.org/journal

Experimental study on the stress wave attenuation effect of filled cracks in rocks under confining pressure

LIU Xin, XU Hong-fa, FAN Peng-xian, GENG Han-sheng, MO Jia-quan, WANG De-rong

State Key Laboratory of Disaster Prevention and Mitigation of Explosion and Impact, Army Engineering University of PLA, Nanjing, Jiangsu 210007, China

Abstract: To study the effectiveness of filled cracks as a means of anti-blasting and wave-elimination for underground protective structures, 36 one-dimensional impact tests were carried out on the intact rock specimens and rock specimens with filled cracks using the SHPB apparatus. The transmittance, stress wave velocity and peak stress value of the specimen under different working conditions were obtained. The impacts of confining pressure level, filling thickness and filling material types on stress wave attenuation were analyzed. The results show that, with the increase of the thickness of the filled cracks, the transmittance of the specimen, stress wave velocity, and stress wave peak stress attenuate clearly. The greater the thickness of the filled crack, the smaller the transmission energy of the stress wave during the propagation process. With the increase of confining pressure, the wave- eliminating effect of filled cracks is reduced due to the closure of pores, but still demonstrate stress wave attenuation effect to some extent. Therefore, using particles with higher compressive strength as crack-filling material and increasing filling thickness can effectively improve the wave-eliminating effect in engineering protection.

Keywords: filled cracks; confining pressure; SHPB; stress wave; attenuation

1 Introduction

During an underground explosion, the energy of the explosion stress wave attenuates with propagation. At a certain distance from the explosion center, the shock wave in the rock mass will be transformed into stress wave[1]. There are many structural surfaces such as joints and faults in the natural rock mass. These discontinuities can relatively weaken the propagation of the stress wave[2]. The attenuation effect of structural surfaces is influenced by a series of factors such as the thickness of the discontinuous surface, the nature of the filled cracks, and the in-situ stress. For underground protection engineering, the weakening effect of the leaning structural surface in the surrounding rock (the normal direction of which is close to the stress propagation direction) on the propagation of the explosive stress wave is conducive to the safety of the structure[3–4]. The construction of filled cracks in the surrounding rock of the protective structures is a meaningful countermeasure. The experimental study of the interaction between filled cracks and stress waves in surrounding rock under different confining pressures and the attenuation effects of stress waves when passing through filled cracks are of great significance to underground protection engineering.

The interaction of stress waves with joints and cracks have been studied extensively while the relevant effects of stress waves when passing through the discontinuities were previously analyzed. For example, Liu et al.[5] studied the oblique incidence problem of nonlinear parallel joints and found that the change of stress wave energy is related to the stiffness and spatial distribution of the joints. Li et al.[6–7] used the viscoelastic model and the linear elastic thin-layered model to study the effect of the crack depth on the stress wave propagation assuming that the stress and displacement on both sides of the filled crack are continuous. In addition, according to the momentum conservation of the wave front and the discontinuous displacement method on both sides of the joint, an equation is established describing the propagation of the explosion-induced stress wave obliquely entering the linear elastic joints. Wang et al.[8] started with different types of incident waves and studied the transmission behavior of stress waves at joints. Yu et al.[9–10] studied the influence of joints with different degrees of nonlinearity on the propagation of longitudinal waves. Fan et al.[11] proposed a non-linear viscoelastic equivalent medium model and studied the propagation and change of P waves through a group of parallel jointed rock masses. Zhang et al.[12] found that the existence of joints reduces the amplitude of transmitted waves, and the weakening of the stress wave transmission capacity of joints is related to the phenomenon of joint surface damage. Yang et al.[13] used discrete element software UDEC to simulate the propagation of stress waves in inclined joints and cracks, then calculated the transmission and reflection coefficients. Schoenberg[14] and Pyrak-Nolte et al.[15] used linear elastic joint displacement discontinuity models to derive the analytical solutions of the transmission and reflection of one-dimensional stress waves entering a single joint at any angle.

Since joints and cracks in rock mass often contain impurities, when stress waves pass on in filled cracks, factors such as the physical and mechanical properties of the filling material within the cracks, and the porosity of the filling material have a prominent impact on the

Received: 12 January 2021 Revised: 27 March 2021
This work was supported by the National Natural Science Foundation of China (51979280, 11772355) and the Natural Science Foundation of Jiangsu Province (BK20190572).
First author: LIU Xin, male, born in 1991, PhD candidate, focusing on anti-blast structure of underground cavern. E-mail: 844535152@qq.com
Corresponding author: FAN Peng-xian, male, born in 1983, PhD, Associate Professor, research interests: rock mechanics and underground engineering. E-mail: fan-px@139.com

propagation of the waves[16−18]. Due to the complexity of geometric characteristics of actual cracks and their fillings, the problem of the stress wave propagation still requires investigations, and experimental research is the most important research method. Chen et al.[19] investigated by model tests and found that the attenuation degree of the explosive stress wave through the filled joints increases linearly with the increase of the filling medium, and the attenuation rate of the transverse stress wave is greater than that of the longitudinal attenuation. Li et al.[20] experimentally studied the propagation law of stress waves in rock joints filled with sand. Yu et al.[21] studied the propagation of the stress wave in the filled joints by engaging the SHPB device and found that the transmission coefficient is related to the incident angle of the stress wave. Li[22] studied the influence of weak interlayer and interlayer thickness on the propagation of stress waves by means of the equivalent wave impedance method. Li et al.[23] and Wu et al.[24] studied the propagation of stress waves between a single and two filled cracks and found that the properties of the filling material, filling thickness and incident wave properties all have influence over the stress wave transmission coefficient. Xue et al.[25] conducted a study on the attenuation of explosive stress waves through structural surfaces filled with different materials and found that the mud fillings have the largest attenuation, followed by debris filling, and the smallest attenuation is found in the cemented fillings. Ding et al.[26] concluded that the transmission coefficient of the filled joints decreases with the increase of the incident wave frequency. The greater the joint thickness, the more obvious the phenomenon is. Li et al.[27] studied the propagation of P waves in rock cracks filled with quartz sand and found that the thickness of the filled cracks significantly varies the natural frequency of the stress wave.

The above research mainly focuses on the law of transmission and reflection of stress waves when passing through joints and cracks. However, most of the natural joints and cracks exist in the surrounding rock of the excavation, few literatures have analyzed the stress wave propagation problem considering the influence of the in-situ stress of joints and cracks. Although studies have shown that filled cracks and faults can effectively attenuate stress waves[28−29], using propagation attenuation characteristics of the cracks and transforming the knowledge into a technical method for anti-blasting and wave-eliminating in underground engineering are rarely reported. In this paper, filled cracks are regarded as an anti-blasting and wave-eliminating technical means for underground engineering, and SHPB device that can provide confining pressure is used to simulate the wave-eliminating effect of rock-filled cracks under confining pressure. By measuring the transmittance, wave velocity, and peak stress of the specimen under various parameters, the attenuation effect of different working conditions with varying filling material, filling thickness, and confining pressure are analyzed for providing validation for the application of the wave elimination technology.

2 Test method and specimen preparation

2.1 Filled rock specimen

The selected rock is Sichuan red sandstone with a density of 2.4 g/cm^3. The average compressive strength and elastic modulus are 50.0 MPa and 9.5 GPa. The original rock test block is made of intact red sandstone with no cracks, which is prepared by uniformly core-taking, cutting, and polishing. According to the test requirements, cylindrical test blocks with a diameter of 75 mm and thicknesses of 40, 18, 17 and 16 mm, respectively were prepared. The red sandstone test blocks are shown in Fig.1.

Fig. 1 Rock test block

To meet the requirements of the SHPB test for the assumption of specimen uniformity, the particle size of the filling material in the rock cracks should be as small as possible. In addition, for the preset minimum filling interlayer thickness, the particle diameter should not be greater than 4 mm, so the selected white corundum material is manually screened with a standard sieve that has an aperture of 1.18 to 2.36 mm. The density of the white corundum particle is 2.9 g/cm^3. The resin-coated sand filling material is selected with a diameter of about 0.42 mm, and its density is 2.3 g/cm^3. The rubber powder cement mortar with a density of 1.7 g/cm^3 is made of 30% rubber powder and the mixing ratio is cement: water: rubber powder: sand=586:293:450:1 050. The average 28 day's compressive strength of the resulted mortar material is 14 MPa. For the rubber powder cement mortar material, manual grinding process is involved to prepare it into a thin cylindrical sandwich specimen with a diameter of 75 mm and a thickness of 6 mm. Then, the abovementioned materials (rubber powder cement mortar, white corundum, and resin-coated sand) were used as rock cracks-filling interlayer materials, and the cracks-filled interlayer SHPB specimens with a diameter of 75 mm and a total height of 40 mm were made as shown in Fig.2. The height of the test piece is set as h and the thickness of the cracked interlayer as Δ.

(a) Rubber powder cement mortar (b) Resin-coated sand (c) White corundum

Fig. 2 Rock specimens with filled cracks

A total of 12 sets of SHPB tests under triaxial stress were carried out, and each set of tests was carried out 3 times. For different crack filling materials, the experi-

ment considered the influence of changing parameters such as the magnitude of the applied confining pressure and the thickness of the filled cracks. In the SHPB tests, the initial pressure of the bullet chamber is 0.2 MPa to ensure that the initial incident velocity of the bullet is equivalent during the test, so that the magnitude of the stress wave is approximate the same. The specific test conditions are summarized in Table 1.

Table 1 Summary of SHPB tests

Specimen Type	Confining pressure /MPa	Filling thickness /mm
Intact rock	0	0
Intact rock	3	0
Intact rock	6	0
Intact rock	9	0
White corundum particles	0	6
White corundum particles	3	4
White corundum particles	3	6
White corundum particles	3	8
White corundum particles	6	6
White corundum particles	9	6
Resin coated sand	3	6
Rubber powder cement mortar	3	6

2.2 Test device and method

2.2.1 SHPB device

The experiment was carried out on the ϕ75 mm confining pressure SHPB device in Hefei Jiang Hydro Dynamic Mechanics Laboratory. As shown in Fig. 3, the rod is made of steel, the length of the incident rod is 3,500 mm, the length of the transmission rod is 2,000 mm, and the length of bullet is 600 mm. A hydraulic confining pressure device is used to apply axial and circumferential pressure to the test specimen. Two sets of corresponding strain collection points were located on the incident rod and transmission rod. The strain collection point on the first group of incident rods is 1,715 mm away from the incident rod–specimen interface, and the strain collection point on the transmission rod is 675 mm away from the transmission rod–specimen interface. The strain collection point on the second group of incident rods is 1,915 mm away from the incident rod–specimen interface, and the strain collection point on the transmission rod is 815 mm away from the transmission rod–specimen interface. The strain signal is collected and recorded by a semiconductor strain gauge. The strain gauge amplification factor is 110, and the resistance is 120 Ω. Two strain gauges are symmetrically attached to each strain collection point. After connecting in series, it is connected to a Wheatstone bridge and is amplified and processed by a strain gauge and an oscilloscope. At the same time, to satisfy stress balance and uniform deformation, a rubber sheet shaper is attached onto the front end of the incident rod.

2.2.2 Test methods

In the test, different levels of confining pressures are applied to the predetermined test specimen through a hydraulic confining pressure chamber. The effect of filled crack specimen on stress wave attenuation under compressive conditions is mainly measured by the transmittance of the specimen, as well as the wave velocity and the peak stress in the specimen.

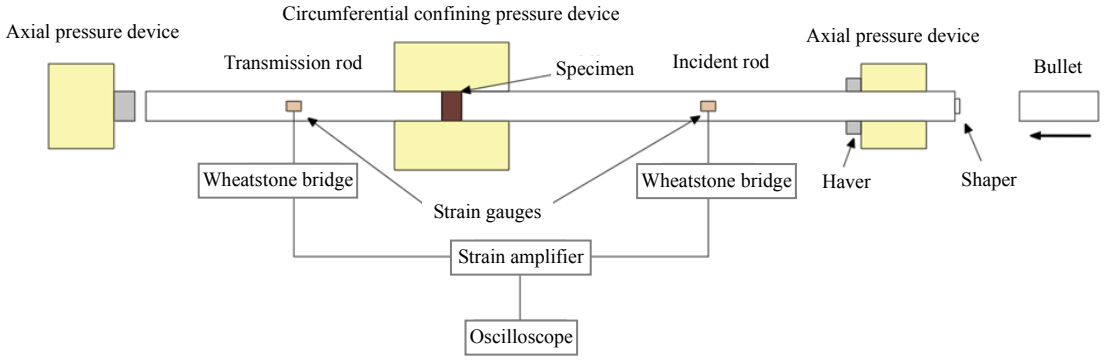

Fig. 3 Schematic of a SHPB apparatus

In the SHPB test, the bullet hits the incident rod to form a one-dimensional compression wave in the incident rod, and the generated wave propagates along the incident rod. When the compression wave passes through the specimen between the incident rod and the transmission rod, part of the compression wave is reflected to form a reflected wave at the junction of the incident rod and the specimen due to the different wave impedances. The rest of the compression wave continues to propagate along the transmission rod and then forms a transmitted wave. The magnitude of the transmitted wave in the transmission rod were used to explore the attenuation of the stress wave in each specimen. According to the incident and transmission data set of each channel stored in the oscilloscope, the peak voltage *u* is taken as the main calculation parameter. Since the total length of the SHPB specimen is 40 mm, the dimensionless transmission coefficient of the specimen ρ is defined as

$$\rho = \frac{u_0 F_0}{u_1 F_1} \tag{1}$$

where u_0 is the peak value of the stress wave transmission voltage; u_1 is the peak value of the stress wave incident voltage; F_0 is the transmission calibration coefficient; F_1 is the incident calibration coefficient. The calibration coefficients are determined by SHPB testing without involving test pieces. According to the dimensionless transmission coefficient ρ, the values of the stress wave transmitted and reflected when the stress wave passes through the test piece can be quan-

titatively determined, and consequently the attenuation effect of the test piece under different working conditions can be intuitively quantified.

In the experiment, the stress wave velocity can be calculated by dividing the propagation distance by the propagation time. The specific measurement method is as follows: two monitoring points are set on the incident rod and transmission rod, respectively to record the starting point of the incident and transmitted waves. The starting time indicates the moment that stress wave propagates to the position of the strain gage. The time difference between the incident and transmission rods is the total time used by the stress wave to propagate within this distance, denoted as t_0. This time is composed of three parts: the time t_R denotes the travelling time in the incident rod; the time t_T denotes the travelling time in the transmission rod; and the time t denotes the travelling time in the specimen. Since the propagation distance in the incident rod and the transmission rod is known, and the wave velocity of the stress wave in the rod is known, so the value of t_R, t_T can be calculated while t_0 is measured. Thus, the propagation time of the stress wave in the specimen t can be obtained. Based on the thickness of the test piece, the wave propagation velocity in the test piece can then be calculated. The specific wave velocity calculation diagram is shown in Fig.4.

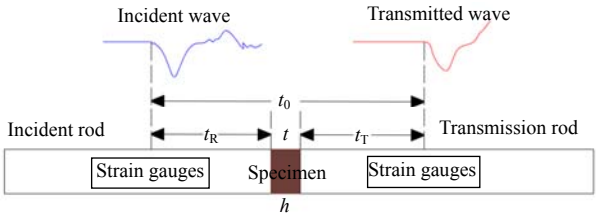

Fig. 4 Schematic of stress wave velocity calculation

The specific calculation formula of the wave velocity in the specimen is as follows:

$$C = \frac{h}{t} = \frac{h}{t_0 - t_R - t_T} \tag{2}$$

where t_R is the time for the stress wave to propagate from the incident rod strain gauge to the incident end face of the specimen; t_T is the stress wave from the transmission end face of the specimen to the transmission rod strain gauge; t is the wave propagation time in the specimen; and h is the height of the specimen.

In the test, the instantaneous maximum pressure generated in the test piece by the bullet hitting the incident rod is called the peak stress of the test piece. According to the peak stress under different working conditions, the wave-elimination performance of the filled crack can be quantitatively analyzed. This paper uses the software PHSICAL developed based on the three-wave phenomenon in the SHPB test to obtain the peak stress in the specimen. The software converts the measured strain voltage signal data to calculate the peak stress in the specimen. The incident and transmitted wave voltage data files are input, then the baseline of the incident and transmitted waves is adjusted while the division time point is determined, and then the peak stress in the specimen can be obtained.

3 Test results and analysis

According to the established working conditions, 36 SHPB tests under variable confining pressures were carried out. Among them, tests on intact rock specimens without any cracks were performed 12 times, numbered A1–A12, to establish a comparison baseline. Under a confining pressure of 3 MPa, three different filling materials were organized in the order of white corundum particles, resin-coated sand, and rubber powder cement mortar. The test pieces with the filling thickness of 6 mm were carried out three times in each group, numbered B1–B9. Under a confining pressure of 3 MPa, two sets of test pieces filled with white corundum particles in the thickness of 4 and 8 mm were carried out three times in each group, numbered C1–C6. Each group of test pieces filled with white corundum particles with a thickness of 6 mm at a confining pressure of 0, 6 MPa and 9 MPa was carried out three times, numbered D1–D9.

3.1 Typical SHPB curve of rock-filled cracks

Figure 5 is a summary diagram of the typical voltage signal curves of the filling material specimen shown by the oscilloscope in the SHPB test. The solid lines are the incident wave curves and their reflected wave curves, and the lines with hollow circle (hollow triangle, hollow square) are the transmitted wave curves. It can be seen that the incident wave curves of different specimens are almost overlapped, and the subtle differences are due to the subtle difference of bullet impact speeds, which implies that the loading conditions of the specimens are basically the same. Under a given confining pressure, due to the difference of the filling material, the amplitudes of the reflected wave and the transmitted wave demonstrate significant changes. In the figure, the intact rock has the largest peak value of the transmitted wave and the smallest peak value of the reflected wave. It shows that the intact rock has a weaker ability to reflect stress waves. Among the crack-filled specimens, the wave peaks of the white corundum-filled cracked specimens and other crack-filled specimens are reduced to a considerable extent compared with the intact rock, and the reflected wave peaks gradually become larger. Therefore,

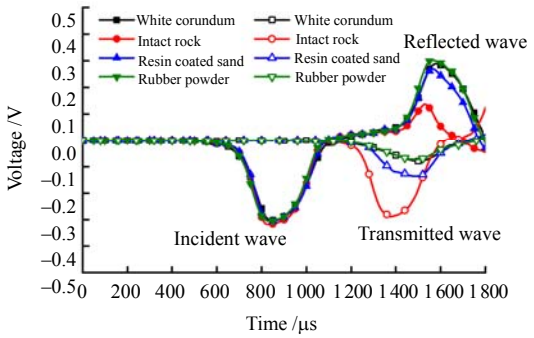

Fig. 5 Typical voltage signal curves

under the action of confining pressure, the filled crack specimen can reflect most of the energy of the stress wave, and has a good energy attenuation effect on the stress wave.

After necessary calculations, the test results of transmittance, stress wave velocity and peak stress of all specimens are listed in Table 2.

Table 2 Test results

Specimen number	Confining pressure /MPa	Filling thickness /mm	Dimensionless transmittance /%	Stress wave velocity /(m·s^{-1})	Peak stress /MPa
A-1	0	—	86.67	1 101	102.7
A-2	3	—	89.19	1 445	111.2
A-3	6	—	91.26	2 177	106.0
A-4	9	—	92.90	3 151	111.8
A-5	0	—	84.86	978	105.9
A-6	3	—	88.91	2 000	105.7
A-7	6	—	91.25	2 536	109.8
A-8	9	—	91.46	3 636	105.5
A-9	0	—	88.55	1 052	100.9
A-10	3	—	92.12	1 576	103.7
A-11	6	—	94.47	2 605	101.9
A-12	9	—	94.77	2 485	101.6
B-1	3	6	29.82	816	30.4
B-2	3	6	37.02	689	39.1
B-3	3	6	38.96	606	33.6
B-4	3	6	59.55	816	57.3
B-5	3	6	42.07	833	51.2
B-6	3	6	46.27	727	56.0
B-7	3	6	37.80	449	29.0
B-8	3	6	36.54	350	32.0
B-9	3	6	57.45	320	60.3
C-1	3	4	44.71	975	43.4
C-2	3	4	40.99	930	41.8
C-3	3	4	45.27	1 052	39.6
C-4	3	8	24.82	344	27.6
C-5	3	8	30.50	363	30.7
C-6	3	8	26.21	430	23.9
D-1	0	6	15.47	167	17.4
D-2	0	6	16.43	155	16.2
D-3	0	6	17.76	130	20.7
D-4	6	6	49.37	829	32.2
D-5	6	6	47.54	771	36.5
D-6	6	6	48.62	1 028	45.9
D-7	9	6	58.66	2 761	51.3
D-8	9	6	36.93	2 111	49.3
D-9	9	6	45.20	2 509	52.9

For underground explosions in rock and soil, with increase of the explosion equivalent and propagation distance, the wavelength of the ground shock increases, and the influence of rock mass cracks and inhomogeneities decreases. The impact attenuation of discontinuous surfaces such as rock joints and cracks can be roughly evaluated by the ratio of the wavelength to the thickness of the discontinuity. If the explosive equivalent is large and the positive pressure action time of the ground impact lasts for a long time, the discontinuous surface must have a certain thickness to achieve a better anti-explosion and wave elimination effect.

The wavelength of the ground impact of a nuclear explosion is mainly related to the explosion equivalent and the propagation distance[30]. In general, the wavelength of the explosive ground impact has a linear relationship with the propagation distance. At the same time, as the propagation distance increases, the peak of the shock wave overpressure decreases and gradually moves to the tail. Outside the inelastic deformation zone, the ratio of the waveform boost time to the positive pressure rise time can reach 1:3–1:2, which is close to the incident wave of the SHPB pressure bar.

Assuming that the buried depth of the project is on the order of hundreds of meters, and the thickness of the artificial crack layer is 0.2 to 1.0 m, the ratio of wavelength to thickness used in the test is basically equal to or slightly smaller than that of the actual project. From the views of waveform as well as the ratio of wavelength to thickness, using SHPB test to simulate the interaction between real explosive ground impact and cracks has good similarity.

3.2 The influence of filling material on the attenuation of stress wave

Figure 6 shows the transmittance, wave velocity, and peak stress histograms of specimens filled with different materials in the cracks. The confining pressure level of the specimens is 3 MPa, and the thickness of the filled cracks is 6 mm. It illustrates that the transmittance, wave velocity, and peak stress of the specimens in all groups are greatly reduced as compared with the intact rock.

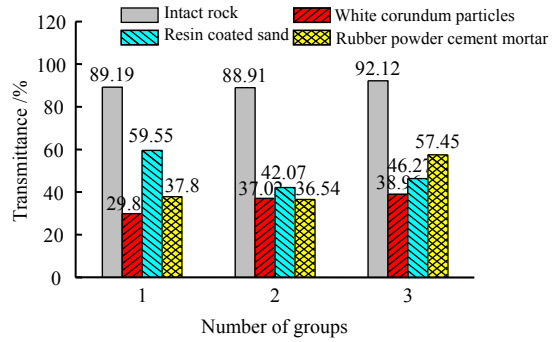

(a) Stress wave transmittance of filled cracks with different materials

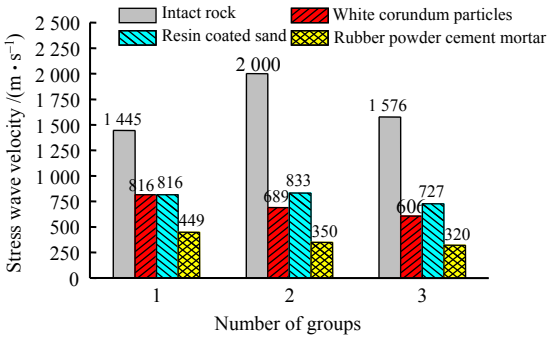

(b) Stress wave velocities of filled cracks with different materials

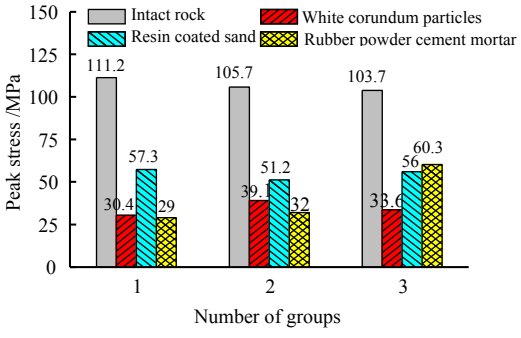

(c) The peak stress of the stress wave of filled cracks with different materials

Fig. 6 Characteristic parameters of specimens with different crack filling materials

To accurately reflect the attenuation of the stress wave caused by the filled cracks, the average result of the three tests under the same working condition is taken and the relative attenuation ratio of each parameter is calculated using the intact rock specimen as a reference. The calculation results are summarized in Table 3. The average transmittance of the intact rock specimens is 90.07%, which is about 2.5 times the average transmittance (35.27%) of the specimens filled with white corundum particles, so the relative attenuation ratio of the white corundum particles is as high as 60.84%. In the specimens filled with white corundum particles, the average peak stress is 34.37 MPa, which is only 32% of the average peak stress of 106.87 MPa in the intact rock specimen, and the relative attenuation rate is also as high as 67.84%. When filled with other materials, the stress wave transmittance, propagation velocity and peak stress of the stress wave are also reduced by about 45% to 77%. Therefore, the filled crack in the rock has a strong weakening effect on the propagation of the stress wave. Meanwhile, when comparing the above histograms, the white corundum particles have a better wave-eliminating effect than the resin-coated sand particles from the perspective of transmittance, wave velocity and peak stress. This is because the particle size of the white corundum particles selected in the experiment is slightly larger than the particle size of the resin-coated sand. At the same time, the void ratio between the particles is larger in white corundum, which leads to the increase of reflection and refraction during the propagation of the stress wave as well as the increase of the energy attenuation effect, these result in a significant decline in the value of each representative parameter of the stress wave. While the finer resin-coated sand has a smaller void ratio under the action of confining pressure, which leads to a slightly compromised wave-eliminating effect. The attenuation effect of the stress wave of the rubber powder cement specimen is also considerable, especially for the attenuation of the wave velocity, which reaches 77.71%, being the most significant among the three filling materials.

Table 3 Average testing values and relative attenuation ratio

Specimen type	Mean value	Transmittance		Wave velocity		Peak stress	
		Value /%	Attenuation ratio /%	Value /(m·s^{-1})	Attenuation ratio /%	Value /MPa	Attenuation ratio /%
Intact rock	Reference value	90.07	—	1 674	—	106.87	—
White corundum particles	Mean value of test	35.27	60.84	704	57.98	34.37	67.84
Resin-coated sand	Mean value of test	49.30	45.26	792	52.68	54.83	48.69
Rubber powder cement mortar	Mean value of test	43.93	51.22	373	77.71	40.43	62.17

3.3 Influence of filling thickness on attenuation of stress wave

Figure 7 presents the transmittance curves of specimens with different filling thicknesses by using white corundum as the crack filling material. The horizontal axis is the ratio of the filling thickness Δ to the height h of the specimen. The vertical axis is the dimensionless transmittance ρ. The confining pressure of the specimens is 3 MPa. The transmittance of the filled cracks specimens gradually decreases with the increase of the filling thickness, and the transmittance attenuation is extremely obvious. When the filling thickness is 8 mm, the transmittance of the specimen drops from 90% of the intact rock to about 30%. In addition, the curvilinear correlation between the transmittance and the thickness of the specimen tends to gradually flatten up.

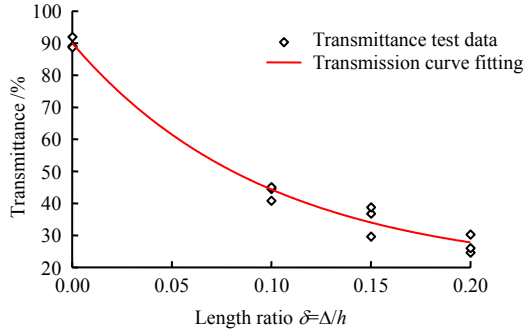

Fig. 7 Specimen transmittance under different crack filling thicknesses

When the stress wave passes through the filled crack, some part of it is reflected at the interface, another part is dissipated in the process of compression deformation of the filling material and particle slip, and the rest part propagates along the force chain skeleton of the filling material and transmitted to the back of the filled crack. When the thickness of the crack increases, the distance traveled through the filling material increases, and the dissipated energy increases, thereby causing a decrease in transmittance. It can be seen from the test results that when the ratio of the crack thickness to the total length of the specimen is small, the attenuation of the stress wave parameter is very sensitive to the thickness of the filled crack. As the filling thickness increases, the slope of the attenuation curve becomes flatter and gradually approaches a stable value (The corresponding values of filling materials). This phenomenon reminds that in actual engineering, the crack is not always the thicker the better, instead it is necessary to comprehensively evaluate factors such as the wave-absorbing benefits, the risk of surrounding rock stability, and the engineering cost.

It can be seen from Fig.7 that the dimensionless transmittance ρ has a good correlation with the ratio of the thickness of the filled cracks and the height of the specimen $\delta(\Delta/h)$, and it approximately obeys the law of exponential decay:

$$\rho = \rho_r e^{\delta^{A_2} \ln(\rho_t/\rho_r)} \quad (3)$$

where δ is the crack filling length ratio, which is the

ratio of the thickness of the filled crack Δ to the height of the specimen h and satisfies the relationship $0 \leqslant \delta \leqslant 1$; ρ is the transmittance of the specimen; ρ_r is the transmittance of the intact rock (that is the transmittance when δ equals 0); ρ_i is the transmittance of the interlayer (that is the transmittance when δ equals 1); λ is the transmittance attenuation coefficient related to the filling material.

By fitting the test data shown in Fig. 7, the transmittance parameter values of the test specimen with white corundum particles interlayered are as follows: $\rho_r = 90$, $\rho_i = 1.68$, $\lambda = 0.75$. The fitting correlation coefficient R^2 is 0.99.

Figures 8 and 9 correspond to the stress wave velocity curve and the peak stress curve of the stress wave. The horizontal axis is the ratio of the thickness of the filled crack to the length of the specimen, and the vertical axis is the stress wave velocity V and the peak stress P of the stress wave. The confining pressure is 3 MPa. As shown in the figure, both the stress wave velocity and the peak stress show a correlation with the thickness of the filled cracks. With the increase of the thickness, the stress wave velocity and peak stress show a similar change pattern as the transmittance, so exponential function equations are used to fit the stress wave velocity and peak stress curves. The fitting curves are shown in Figs.8 and 9, and the fitting equations are given as

$$\left.\begin{aligned} V &= V_r e^{\delta^{\lambda_1} \ln(V_i/V_r)} \\ P &= P_r e^{\delta^{\lambda_2} \ln(P_i/P_r)} \end{aligned}\right\} \quad (4)$$

where V is the stress wave velocity; V_r is the stress wave velocity of the intact rock (that is the stress wave velocity when δ equals 0); V_i is the interlayer stress wave velocity (that is the stress wave velocity when δ equals 1); λ_1 is the wave velocity attenuation coefficient related to the filling material; P is the peak stress; P_r is the peak stress of the intact rock (that is the peak stress when δ equals 0); P_i is the peak stress of the interlayer (that is the peak stress when δ equals 1); and λ_2 is the peak stress attenuation coefficient related to the filling material.

By fitting the test data shown in Fig. 8 and Fig. 9, the wave velocity parameter values of the white corundum particle interlayer specimen are as follows: $V_r = 1\,897$, $V_i = 0.64$, $\lambda_1 = 1.18$, and the fitting correlation coefficient R^2 is 0.9. The peak stress parameter values of the specimen are as follows: $P_r = 106$, $P_i = 0.18$, $\lambda_2 = 0.9$, and the fitting correlation coefficient R^2 is 0.99.

In the fitting curves, the stress wave velocity decays fastest with increasing thickness of the filled cracks. When the stress wave propagates in an 8 mm filled crack, its peak stress is reduced to about 27.4 MPa, which is 74% less than the peak pressure in the original intact rock. Comparing the attenuation coefficients of the transmittance, stress wave velocity and peak stress of the stress wave in the specimen under a variable filling thickness, the relationship satisfies the equation: $|\lambda| < |\lambda_2| < |\lambda_1|$. Among the three parameters, the stress wave velocity attenuation coefficient is the largest, and is the most sensible to the change of filled crack thickness.

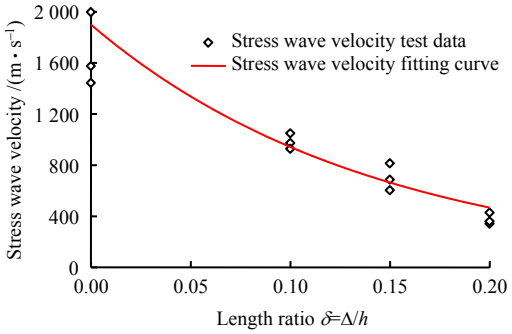

Fig. 8 Stress wave velocity at different crack filling thicknesses

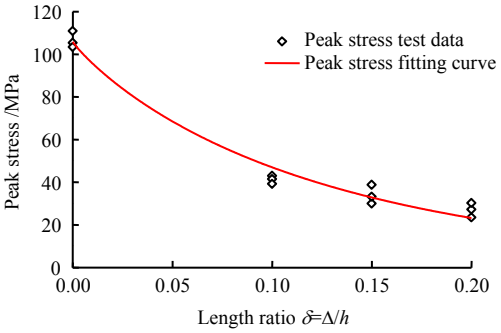

Fig. 9 Peak stress of specimen at different crack filling thicknesses

3.4 The influence of rock filled cracks on the attenuation of stress wave under different confining pressures

The transmittance curve of the specimen with 6 mm filled cracks and the transmission loss of the intact rock are plotted in Fig.10 under different confining pressures. The horizontal axis is the confining pressure, and the left vertical axis is the dimensionless transmittance ρ. To better study the influence of confining pressure in the intact rock on the transmittance, the right vertical axis is set as the transmittance loss of the intact rock specimen with changing confining pressures. It can be seen that the transmittance of the filled cracks specimen increases with the increase of the confining pressure, but the increasing trend gradually slows down, which demonstrates the same trend as that of the intact rock transmittance with the confining pressure.

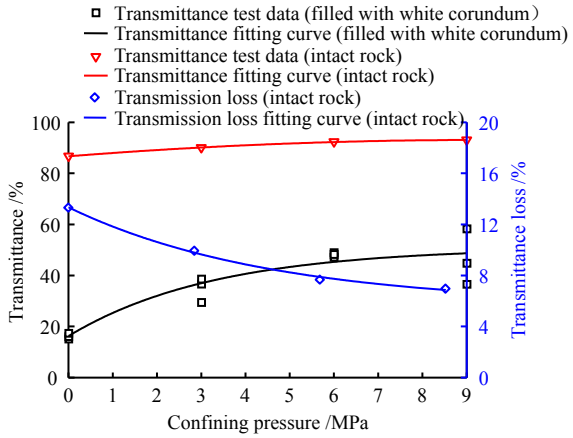

Fig. 10 Transmittance and transmittance loss of specimen under different confining pressures

Through fitting the dimensionless transmittance ρ and the confining pressure σ, it is found that there is a good correlation that basically obeys an exponential growth and approaches to a fixed value, as shown in the following formula:

$$\rho = \rho_1 + \rho_2 e^{\gamma\sigma} \tag{5}$$

Where: ρ_1 and ρ_2 are the parameters related to the transmittance of the specimen, $(\rho_1 + \rho_2)$ is the overall transmittance of the specimen without confining pressure; γ is the transmittance growth coefficient related to the interlayer.

Through the fitting analysis of the test data shown in Fig.10, the transmittance parameter values of the specimen with white corundum particles are as $\rho_1 = 51$, $\rho_2 = -34.7$, $\gamma = -0.3$, and the fitting correlation coefficient R^2 is 0.91.

From Fig. 10, it shows that with the increase of the confining pressure, the transmittances of the intact rock specimen and the specimen filled with cracks increase correspondingly, and the increment of the transmittance of the filled cracks is greater than that of the intact rock specimen. The reason is there are many pores between the particles of the filling materials, and under the action of the confining pressure, the pores are gradually closed, and the diffraction and reflection phenomena of stress waves are reduced when the stress waves propagate through the cracks, therefore the overall pass-through ability is increased, which leads to an increase in transmittance. However, the transmittance of the specimens filled with cracks tends to gradually slow down with the increase of confining pressure. This is because the internal void of the filled cracks gradually closes and disappears with the increase of confining pressure, so the transmission rate of the whole specimens will approach a peak value and stop growing. The maximum confining pressure applied in this test is 9 MPa. This level of confining pressure is not enough to damage the rock or the filling material to form new micro-cracks and structural surfaces. Assuming that the confining pressure increases to the crack initiation stress of rock, new micro-cracks will sprout in the rock itself, the transmittance may show a small decrease as the confining pressure increases. In the tested working conditions, the porosity of the intact rock is very low, and the tiny cracks tend to be closed under higher confining pressure, so the transmittance of the intact rock increases slightly, while the transmittance loss is correspondingly reduced. Furthermore, the energy of the stress wave is greater which indicates that the energy absorption effect in the intact rock begins to weaken when the confining pressure increases.

Figures 11 and 12 are the stress wave velocity curve and the peak stress curve of the specimen under variable confining pressures. From Figs.11 and 12, the stress wave velocity and peak stress also show a trend similar to that of the transmittance with increasing confining pressure, but the growth rates are different. The wave velocity of the specimen shows an increasing trend with increasing confining pressure, and the rate of increase is faster than that of the peak stress. When the confining pressure increases from 0 MPa to 9 MPa, the wave velocity of the stress wave in the specimen increases from 187 m/s to about 2 500 m/s, which is close to the stress wave velocity in the intact rock while the peak stress increases from about 20 MPa to about 46 MPa. The stress wave velocity in the specimen filled with cracks is more sensitive to the change of confining pressure than the peak pressure.

The accelerated growth of the wave velocity in the specimens with the increase of confining pressure revealed by the experiment may be related to the compaction and deformation mechanism of the granular materials under different confining pressures. When the confining pressure is low, the initial force between the particles is small. Under the action of sudden stress fluctuations, the particles are prone to redistribute their position and reorganize the force chains. When the confining pressure increases, the interaction and interlock among the particles will be reinforced. The confining effect causes more particles to be restrained near the initial position and can only perform small translation and rotation. Under the action of higher confining pressure, some particles may be broken. This complex deformation mechanism has been found in the short-term, mid-term even long-term deformation of quartz sand and coral sand[31], which may be potentially causing the accelerated growth trend of the stress wave velocity of the specimen as the confining pressure increases.

With the help of the exponential function growth expression, the stress wave velocity and peak stress curves in the filled cracks are fitted:

$$\left.\begin{aligned} V &= V_1 + V_2 e^{\gamma_1\sigma} \\ P &= P_1 + P_2 e^{\gamma_2\sigma} \end{aligned}\right\} \tag{6}$$

where V_1 and V_2 are the parameters related to the wave velocity of the specimen, $(V_1 + V_2)$ is the wave velocity of the specimen filled with cracks when confining pressure has not been applied; γ_1 is the wave velocity growth coefficient related to the interlayer; P_1 and P_2 are the parameters related to the peak stress of the specimen, $(P_1 + P_2)$ is the peak stress of the test specimen when confining pressure has not been applied; and γ_2 is the peak stress growth coefficient related to the filled interlayer.

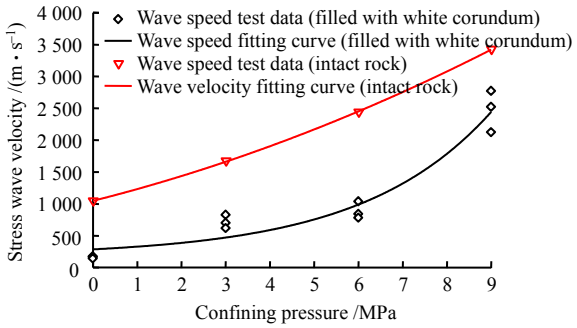

Fig. 11 Stress wave velocity in specimen under different confining pressures

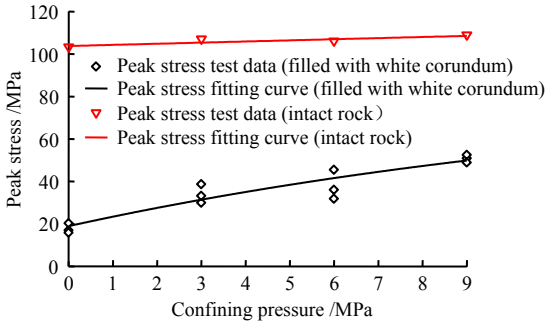

Fig. 12 Peak stress of stress wave under different confining pressures

By fitting the test data shown in Figs. 11 and 12, the wave velocity parameter values of the test piece with white corundum particles are as $V_1 = 183$, $V_2 = 103$, $\gamma_1 = 0.34$, and the fitting correlation coefficient R^2 is 0.94. The peak stress parameter values of the specimen are as $P_1 = 86.7$, $P_2 = 68$, $\gamma_2 = -0.07$, and the fitting correlation coefficient R^2 is 0.92.

By comparing the fitting equations for the transmittance, wave velocity and peak stress of the specimen under different confining pressures, it is found that the growth coefficient of each parameter satisfies the relational formula $|\gamma_2| < |\gamma| < |\gamma_1|$. This relation is similar to that of the attenuation coefficient when the thickness of the filled crack is changed. The growth coefficient of the wave velocity is still the largest, which indicates that the wave velocity in the filled crack is greatly affected by the confining pressure. In addition, the growth coefficient of stress wave velocity is positive, while the growth coefficients of transmittance and peak stress are negative. This is because when the filled crack is subjected to confining pressure, the stress wave velocity is greatly affected by the void ratio, and the wave velocity in the specimen increases rapidly with the closure of the pores. From the above fitting curve, when there are filled cracks in the rock, on the one hand, the tiny cracks and small voids inside the rock are going to close with the application of the confining pressure; on the other hand, the internal voids of the filling particles are also gradually reduced by the confining pressure, and the overall contact stiffness between particles increases, which leads to an increase in the transmittance of the stress wave as well as an increase in the wave velocity of the stress wave. Under the action of confining pressure, the internal voids of the specimen are greatly reduced, and the penetrating energy of the stress wave increases, resulting in an increase in the peak pressure. However, compared with the original intact rock, the peak pressure in the filled crack specimen is 51.2 MPa at a confining pressure of 9 MPa, which is only half that of the intact rock. As the confining pressure increases, the peak stress of the specimen continues to increase but grows at a slower pace. It can be inferred that the peak pressure in the specimen will not increase endlessly with the increase of confining pressure. When the confining pressure increases to a certain extent, the compressibility of the filled particles will be exhausted, the stiffness reaches the maximum, and the tiny cracks in the rock are completely closed, the peak stress of the stress wave will reach the maximum and remain unchanged. Therefore, even in the face of various pressure levels, the interlayer of filled cracks can still provide greater wave attenuation effect comparing to the intact surrounding rock. It is feasible to use filled cracks as a wave-elimination protection method in the surrounding rock of deep-buried protection structures.

4 Conclusion

By using a SHPB device providing confining pressure, the attenuation of stress wave transmittance, wave velocity and peak stress in the rock-filled crack specimen are investigated. The effects of the confining pressure, filling thickness and different filling materials are analyzed. The main conclusions are summarized as follows:

(1) The cracks filled with different materials can significantly attenuate the stress wave transmittance, stress wave velocity and peak stress wave. When the filling thickness is 6 mm and the confining pressure level is 3 MPa, the average relative attenuation ratio of each parameter is between 40% and 80% as compared with the intact rock. The white corundum particles have the best attenuation effect on the peak stress of the stress wave, and the rubber powder cement mortar attenuates the velocity of stress wave most significantly.

(2) As the thickness of the filled crack increases, the refraction and reflection of the stress wave increase while propagating in the filled crack, and the attenuation degree of the stress wave related parameter increases, but the attenuation effect gradually slows down.

(3) As the confining pressure increases, the relevant parameters of the stress wave after passing through the filled cracks are improved. When the confining pressure is 9 MPa, the transmittance and the peak stress wave are only about 50% of the intact rock, except for that the wave velocity gradually approaching the wave velocity of the intact rock. The results indicate that even under high confining pressure, the filled cracks still display a good wave-eliminating ability.

(4) Based on this experiment, the transmittance, stress wave velocity and peak stress curves of the stress wave passing through the rock filled crack are fitted exponentially, and the attenuation law of the stress wave propagation in the filled crack under confining pressure is obtained.

In summary, artificially filled cracks in the surrounding rock have potential application prospects as a means of anti-blasting and wave-elimination in protection engineering. In the case of large burial depth, pressure-resistant crack-filling materials can be used to prevent the closure of artificial cracks. In addition, the thickness of the filled cracks can be properly increased to improve the effectiveness of wave-elimination. However, in actual engineering, the influence of filled cracks on the stability of the surrounding rock of the cavern cannot be ignored.

References

[1] REZAEI NIYA S M, SELVADURAI A P S. Correlation of joint roughness coefficient and permeability of a fracture[J]. International Journal of Rock Mechanics and Mining Sciences, 2019, 113: 150–162.

[2] YU Jin, QIAN Qi-hu, ZHAO Xiao-bao. Research Progress on effects of structural planes of rock mass on stress wave propagation law[J]. Acta Armamentarii, 2009, 30(Suppl.2): 308–316.

[3] WANG Ming-yang, QIAN Qi-hu. Attenuation law of explosive wave propagation in cracks[J]. Chinese Journal of Geotechnical Engineering, 1995, 17(2): 42–46.

[4] WANG Ming-yang, ZHAO Yue-tang, QIAN Qi-hu. Studies on mechanism and quantization of isolation effect of slow angle fault[J]. Chinese Journal of Rock Mechanics and Engineering, 1999, 18(1): 60–64.

[5] LIU Ting-ting, LI Jian-chun, LI Hai-bo, et al. Energy analysis of stress wave propagation across parallel nonlinear joints[J]. Chinese Journal of Rock Mechanics and Engineering, 2013, 32(8): 1610–1617.

[6] LI J C, WU W, LI H B, et al. A thin-layer interface model for wave propagation through filled rock joints[J]. Journal of Applied Geophysics, 2013, 91(4): 31–38.

[7] LI J C, MA G W. Analysis of blast wave interaction with a rock joint[J]. Rock Mechanics and Rock Engineering, 2010, 43(6): 777–787.

[8] WANG Wei-hua, LI Xi-bing, ZHOU Zi-long, et al. Energy-transmitted rule of various stress waves across open joint[J]. Journal of Central South University (Science and Technology), 2006, 37(2): 376–380.

[9] YU Jin, QIAN Qi-hu, SONG Bo-xue, et al. Transmission of various stress waves across multi-fracture with nonlinear deformation behavior[J]. Engineering Mechanics, 2012, 29(4): 1–6.

[10] YU Jin, SONG Bo-xue, QIAN Qi-hu. Propagation of p-waves in dual nonlinear elastic medium for jointed rock mass[J]. Chinese Journal of Rock Mechanics and Engineering, 2011, 30(12): 2463–2473.

[11] FAN L F, MA G W, LI J C. Nonlinear viscoelastic medium equivalence for stress wave propagation in a jointed rock mass[J]. International Journal of Rock Mechanics and Mining Sciences, 2012, 49(1): 11–18.

[12] ZHANG Yu-fei, LI Jian-chun, YAN Ya-tao, et al. Experimental study on dynamic damage characteristics of roughness joint surface based on SHPB[J]. Rock and Soil Mechanics, 2021, 42(2): 491–500.

[13] YANG Feng-wei, LI Hai-bo, LI Jian-chun, et al. Numerical simulation of transmission characteristics of oblique incidence of stress waves across linear elastic joints[J]. Rock and Soil Mechanics, 2013, 34(3): 901–907.

[14] SCHOENBERG M. Elastic wave behavior across linear slip interfaces[J]. Journal of the Acoustical Society of America, 1980, 68(5): 1516–1521.

[15] PYRAK-NOLTE L J, MYER L R, COOK N G W. Transmission of seismic waves across single natural fractures[J]. Journal of Geophysical Research, 1990, 95(B6): 8617–8638.

[16] SHUKLA A, DAMANIA C. Experimental investigation of wave velocity and dynamic contact stresses in an assembly of disks[J]. Experimental Mechanics, 1987, 27(3): 268–281.

[17] AMOS NUR. Effects of stress on velocity anisotropy in rock with cracks[J]. Journal of Geophysical Research, 1971, 76(8): 2022–2034.

[18] HUANG J, LIU X L, ZHAO J, et al. Propagation of stress waves through fully saturated rock joint under undrained conditions and dynamic response characteristics of filling liquid[J]. Rock Mechanics and Rock Engineering, 2020, 53: 3637–3655.

[19] CHEN Xue-feng, ZHAO Xiao-xue, WANG Hai-bo, et al. Model tests and application research on propagation laws of blasting stress wave in jointed and filled rock mass[J]. Journal of Safety Science and Technology, 2018, 14(12): 132–136.

[20] LI J C, MA G W. Experimental study of stress wave propagation across a filled rock joint[J]. International Journal of Rock Mechanics and Mining Sciences, 2009, 46(3): 471–478.

[21] YU J, LIU Z H, HE Z, et al. Fluctuation characteristic test of oblique stress waves in infilled jointed rock and study of the analytic method[J]. Advances in Civil Engineering, 2020(12): 1–12.

[22] LI Xi-bing. Rock dynamics: fundamentals and applications[M]. Beijing: Science Press, 2014: 360–365.

[23] LI J, MA G, HUANG X. Analysis of wave propagation through a filled rock joint[J]. Rock Mechanics Rock Engineering, 2010, 43(6): 789–798.

[24] WU W, LI J C, ZHAO J. Seismic response of adjacent filled parallel rock fractures with dissimilar properties[J]. Journal of Applied Geophysics, 2013, 96(3): 33–37.

[25] XUE Xiao-meng, WANG Jie, CHEN Ji-qiang, et al. Influence of structural planes of rock mass to the blasting stress wave[J]. Metal Mine, 2015(Suppl.1): 36–39.

[26] DING Ying-xun, WANG Zhi-liang, HUANG You-peng. 3D simulation of stress wave propagation in jointed rock mass with filling joint[J], Hydro-Science and Engineering, 2020(6): 80–88.

[27] LI X F, LI H B, LI J C, et al. Effect of joint thickness on seismic response across a filled rock fracture[J]. Geotechnique Letters, 2018, 8(3): 190–194.

[28] FENG X J, ZHANG Q M, MUHAMMAD A. Explosion-induced stress wave propagation in interacting fault system: numerical modeling and implications for chaoyang coal mine[J]. Shock and Vibration, 2019(5): 1–12.

[29] YANG Xin, PU Chuan-jin, LIAO Tao, et al. Effect of prefabricated crack with different fillings on blasting cracks propagation[J]. Explosion and Shocks Waves, 2016, 36(3): 370–378.

[30] QIAN Qi-hu, WANG Ming-yang. Impact and explosion effects in rock and soil[M]. Beijing: National Defense Industry Press, 2010.

[31] WANG J B, FAN P X, WANG M Y, et al. Experimental study of one-dimensional compression creep in crushed dry coral sand[J]. Canadian Geotechnical Journal, 2020, 27(12): 1854–1869.